

## Attomolar Sensitivity in Bioassays Based on Surface Plasmon Fluorescence Spectroscopy

Fang Yu,<sup>†</sup> Björn Persson,<sup>‡</sup> Stefan Löfås,<sup>‡</sup> and Wolfgang Knoll<sup>\*†</sup>

Max-Planck-Institute for Polymer Research, Ackermannweg 10, D-55128 Mainz, Germany, and Biacore AB, Rapskatan 7, SE-754 50 Uppsala, Sweden

Received March 11, 2004; E-mail: knoll@mpip-mainz.mpg.de

Only a high-performance biosensor which is capable of probing trace amounts of analytes in real-time is qualified to fulfill the stringent requirements in diagnosis, drug discovery, proteomics, and the detection of environmentally hazardous compounds, etc. Surface plasmon fluorescence spectroscopy (SPFS) since reported in 1999<sup>1</sup> has the potential to become the method of choice in these applications. In addition to the conventional surface plasmon resonance (SPR) spectroscopy probing of interfacial refractive index changes, SPFS offers the fluorescence signal channel that can directly monitor biomolecular binding kinetics in a highly sensitive way. However, the fluorescence emission from the bound fluorophores encounters significant quenching by metals in short dye-to-metal distances (e.g., <10 nm), which compromises the benefits obtained from the SPR field enhancement. Additionally, a distinct distance-dependent fluorescence profile, originating from the co-effect of the decay of the evanescent surface plasmon field and the metal-induced quenching, suggests a potential signal deviation by, e.g., the unpredictable orientation and/or conformation of the analyte molecules, which is not desirable for practical sensing concerns. The fluorescence profile can be theoretically predicted (cf. Figure 1A) and experimentally depicted with model systems incorporating so-called “surface”<sup>2,3</sup> and “localized”<sup>4</sup> plasmon phenomena, respectively. Efforts have been made in seeking the optimal dye-to-metal distance, e.g., using layer-by-layer strategies.<sup>3,4</sup>

Here, we propose that a spatially extended matrix can be utilized as a binding matrix to overcome these drawbacks of SPFS. The functional chains (e.g., polymer brushes<sup>5</sup>) or networks (e.g., plasma polymerized layers<sup>6</sup>) in the matrix are expected to extend the interaction arena away from the metal, as well as allow for the integration of the fluorescence emission from the fluorophores at different distances from the sensor surface. In this report, a CM5 sensor chip from Biacore is employed, which has gained a significant reputation in the biosensing market since being developed in 1990.<sup>7</sup> Tethered to a self-assembled monolayer (SAM) surface, the carboxymethyl-dextran (CMD) chains extend some 100 nm into the bulk medium, offering numerous carboxylic acid groups ready for the covalent attachment of biomolecules. Although the precise distribution of bound biomolecules along the CMD chains remains unclear, the larger steric hindrance near the tethering point may help to prevent the biomolecules from being too close to the metal. Hence, the layer-architecture matches to the optimal sensing region indicated in theoretical predictions. A model system (cf. Figure 1B) involving a mouse IgG and a fluorophore (Alexa Fluor 647, from Molecular Probes Inc.)-labeled rabbit anti-mouse antibody (AF-RaM, dye-to-antibody ratio = 4.8) as free analyte was employed to demonstrate the limit of detection (LOD) of SPFS.

Mouse IgG was covalently loaded to the CMD matrix following the well-established active ester chemistry<sup>7</sup> with an SPR angle shift

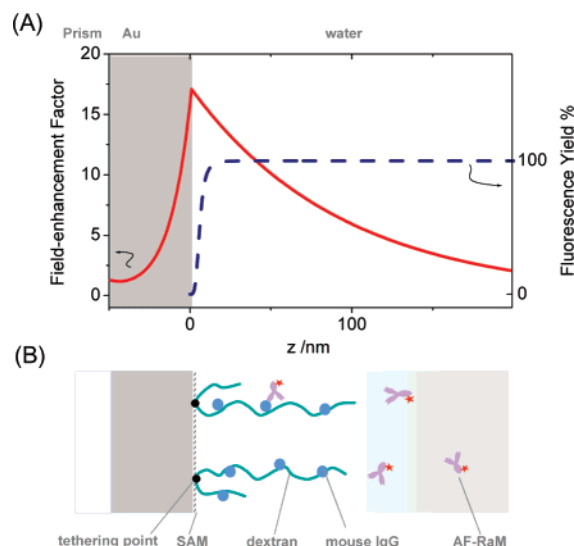


**Figure 1.** (A) The intensity profile of a surface plasmon with the evanescent field extending into the dielectric medium (water) in contact with the metal (Au) layer (solid line), and the fluorescence intensity profile of a fluorophore near a (quenching) metal surface (dashed line). (B) Schematic cartoon of the interfacial architecture of an antibody–antigen interaction in a dextran matrix for LOD evaluation.

of  $\Delta\theta = +1.5^\circ$ . This corresponds to a surface protein density of  $\sigma = 8 \text{ ng mm}^{-2}$ , referring to a correlation of  $\rho = \Delta\theta/\sigma = 0.19 \times 10^9 \text{ deg g}^{-1} \text{ mm}^2$  obtained from a calibration experiment. Figure 2A describes a series of binding assays of AF-RaM samples in a concentration range from 333 aM to 16.7 fM in HBS-EP buffer (Biacore). Each injection of sample solution was followed by a surface regeneration by applying an injection pulse of glycine buffer (10 mM, pH 1.7). At such low analyte concentrations, the binding kinetics of AF-RaM are all firmly controlled by the mass-transport rate from the bulk solution to the interface and can be described by:

$$dR/dt = k_M c_0 \quad (1)$$

indicating that the response  $R$  increases linearly with time  $t$  and the binding slope is proportional to the bulk concentration  $c_0$  of the analyte. The proportionality factor  $k_M$  is known as the mass-transport rate constant. Therefore, plotting the binding slope versus the bulk concentration defines a calibration curve, shown in Figure 2B. The baseline stability was tested by five repetitive injections of mere buffer solutions and the resulting five slopes (of the baseline drift) were analyzed statistically. The sum of the mean plus 3 times the standard deviation (SD) was considered as the baseline signal deviation, which was  $\sim 20 \text{ cps min}^{-1}$ . From the experimental curves in Figure 2A, one can see the following: (1) mass-transport-limited binding signals from all applied concentrations could be resolved

<sup>†</sup> Max-Planck-Institute for Polymer Research.

<sup>‡</sup> Biacore AB.

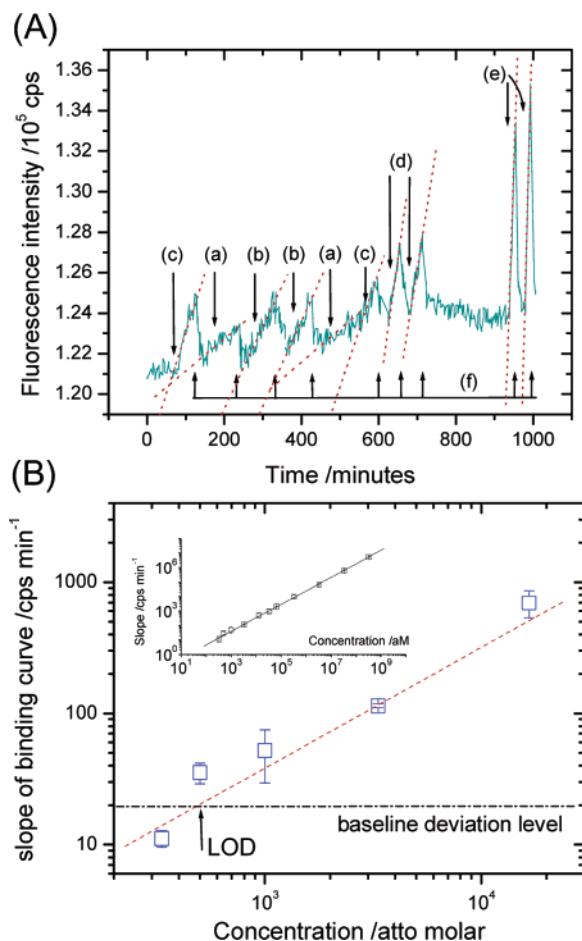


**Figure 2.** (A) Fluorescence response upon the injection of AF-RaM solutions with the concentration of (a) 333 aM, (b) 500 aM, (c) 1 fM, (d) 3.3 fM, (e) 16.7 fM. Regenerations (f) were performed after every sample injection. Dashed lines are the linear fits to the binding curves to yield the corresponding binding slopes. (B) Double-logarithmic plot of the binding slopes obtained from (A), as a calibration curve. The dashed line is a linear fit. The dash-dotted line represents the baseline deviation level, which intersects the calibration curve at  $\sim 500$  aM. The inset summarizes the linear relation between the binding slope of AF-RaM and the concentration over 6 orders of magnitude.

from the baseline, and (2) the regeneration procedures re-set the fluorescence signal to the background level. The resulting dose-response curve intersects with the baseline deviation level, which gives a concentration LOD of  $\sim 500$  aM. It was also demonstrated that the slope of the fluorescence binding signal is a linear function of the AF-RaM concentration over 6 orders of magnitude. (cf. inset of Figure 2B).

In an effort to establish the correlation between the SPR and the fluorescence signals to quantify the number of molecules involved in the binding at the LOD level, a 6.7 nM AF-RaM solution was injected into the flow cell, and the binding was repeatedly paused by temporarily filling the flow cell with HBS-EP buffer. Five angular scans (a, b, c, d, e) were taken at each interval (plotted in Figure 3). It is noteworthy that the dissociation rate of AF-RaM/Mouse IgG ( $k_{\text{off}} \approx 6 \times 10^{-5} \text{ s}^{-1}$ ) was slow enough to ensure a

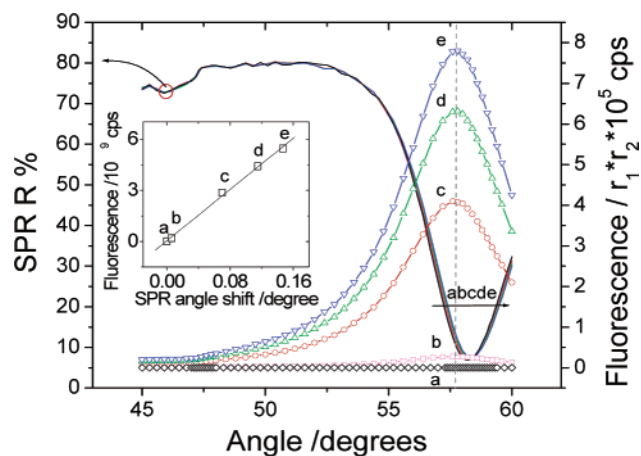


**Figure 3.** Angular scan curves of SPR and fluorescence, at paused stages (a, b, c, d, e) of AF-RaM binding from a 6.7 nM solution. The shift of the SPR minimum angles as well as the increases of the fluorescence signal can be resolved simultaneously. A linear correlation is shown for both signals (cf. the inset). Here, the fluorescence signal was greatly attenuated by lowering the laser intensity (by a factor of  $r_1 = 17$ ) and using a neutral density attenuator (by a factor of  $r_2 = 410$ ) in front of the fluorescence detector, considering the linear working range of the detector (see ref 2 for more experimental details).

negligible loss of AF-RaM during the angular scans (which typically takes  $\sim 120$  s). By plotting the SPR minimum angles versus the peak fluorescence intensities measured, one obtains the slope of  $\sim 3.8 \times 10^{10} \text{ cps deg}^{-1}$  (inset of Figure 3), which corresponds to  $\sim 0.5 \text{ molecule mm}^{-2} \text{ cps}^{-1}$  considering the aforementioned correlation  $\rho$ . Therefore, the LOD (i.e. the baseline deviation of  $\sim 20 \text{ cps min}^{-1}$ ) corresponds to a flux of  $\sim 10$  antibody molecules binding to the sensing area ( $\sim 1 \text{ mm}^2$ ) per every minute. Also, the strictly linear dependence between the SPR and the fluorescence signal may indicate a convoluted distance-dependent fluorescence profile by virtue of the dextran matrix.

In conclusion, a time-resolved ultratrace detection of fluorophore-labeled antibodies has been demonstrated, combining a versatile commercially available sensor chip with a fluorescence-detection unit in the SPFS apparatus. This successful combination offers all the repetitively tested features of the dextran layer and immediately opens a massive amount of sensing opportunities for SPFS. Meanwhile, the documented ability of SPFS to sense a few molecular-recognition and -binding events at the interface strongly suggests its potential in single-molecule sensing, e.g., for implementing an interfacial fluorescence correlation spectroscopy.

## References

- (1) Liebermann, T.; Knoll, W. *Colloids. Surf. A* **2000**, *171*, 115–130.
- (2) Yu, F.; Yao, D.; Knoll, W. *Anal. Chem.* **2003**, *75*, 2610–2617.
- (3) Vasilev, K.; Knoll, W.; Kreiter, M. *J. Chem. Phys.* **2004**, *120*, 3439–3445.
- (4) Malicka, J.; Gryczynski, I.; Gryczynski, Z.; Lakowicz, J. R. *Anal. Biochem.* **2003**, *315*, 57–66.
- (5) Ruhe, J.; Golze, S.; Freidank, D.; Mohry, S.; Klapproth, H. *Abstr. Pap. Am. Chem. Soc.* **2001**, *221*, 321-coll part 1 apr 1.
- (6) Zhang, Z. H.; Chen, Q.; Knoll, W.; Foerch, R.; Holcomb, R.; Roitman, D. *Macromolecules* **2003**, *36*, 7689–7694.
- (7) Löfås, S.; Johnsson, B. *J. Chem. Soc., Chem. Commun.* **1990**, *21*, 1526–1528.

JA048583Q